

Melting at dislocations and grain boundaries: A Phase Field Crystal study

Joel Berry¹, K. R. Elder², and Martin Grant¹

¹ *Physics Department, Rutherford Building, 3600 rue University,
McGill University, Montréal, Québec, Canada H3A 2T8 and*

² *Department of Physics, Oakland University, Rochester, MI, 48309-4487*

(Dated: November 1, 2018)

Dislocation and grain boundary melting are studied in three dimensions using the Phase Field Crystal method. Isolated dislocations are found to melt radially outward from their core, as the localized excess elastic energy drives a power law divergence in the melt radius. Dislocations within low-to-mid angle grain boundaries melt similarly until an angle-dependent first order wetting transition occurs when neighboring melted regions coalesce. High angle boundaries are treated within a screening approximation, and issues related to ensembles, metastability, and grain size are discussed.

PACS numbers: 64.70.D-,61.72.Bb,61.72.Lk,61.72.Mm

Freezing and melting transitions do not exhibit the range of universal behavior associated with continuous phase transitions and largely for this reason have eluded a unified theoretical description. The nature of a given melting transition may depend sensitively on the details of the system and experiment, and can involve many distinct processes both within and between multiple forms of excitations. For example, melting may occur abruptly and discontinuously at the melting temperature T_m , or it may initiate well below T_m at surfaces and/or internal defects and proceed up to T_m . This process of premelting has been studied extensively for surfaces [1, 2] and is relatively well understood, but limited and inconsistent experimental evidence for melting at dislocations and grain boundaries leaves a number of issues unresolved.

A recent study of colloidal crystals has verified that premelting does occur at vacancies, dislocations, and grain boundaries, and has provided measurements of the localized premelting behavior below T_m [3]. The conditions which determine whether premelting will occur continuously or discontinuously, and whether the width of the premelted region diverges are not fully understood. Grain boundaries in Al have been found to liquify very near T_m , and the width of the melted layer appears to diverge [4]. Discontinuous jumps in grain boundary diffusion coefficients [5, 6], mobility [7], and shear resistance [8] have been found in other metals.

Theoretical studies have been based on either explicitly atomistic methods such as Molecular Dynamics [9, 10] and Monte Carlo [11], or on continuum phase field models with uniform phases [12, 13, 14]. In this study, dislocation and grain boundary melting are examined using the Phase Field Crystal (PFC) method [15], which extends the phase field approach to the level of atomistic resolution. This permits straightforward identification of stable equilibrium and metastable non-equilibrium atomic structures, while inherently including crystal symmetry and orientation, elasticity/plasticity, and the individual dislocations which compose the grain boundaries. Our description will be most applicable to

hard-sphere/colloidal systems and possibly simple metals.

The melting behavior of dislocation pairs and symmetric tilt grain boundaries of $\theta = 4^\circ, 8^\circ, 16^\circ, 24^\circ, 32^\circ$, and 44° are examined numerically for a simple PFC model with bcc symmetry. Analytic results are derived for isolated dislocations and low θ boundaries by combining the PFC equations with continuum linear elasticity. A screening approximation is outlined for high angle boundaries, though somewhat surprisingly, the low θ description is found to remain reasonably accurate for high θ .

As shown in reference [16] the PFC free energy can be derived from the Ramakrishnan-Yussouff free energy functional of classical density functional theory [17, 18]. Here we give the final form:

$$F = \int d\vec{r} \left[\frac{B^\ell}{2} n^2 + \frac{B^s}{2} n (2\nabla^2 + \nabla^4) n - v \frac{n^3}{6} + \frac{n^4}{12} \right] \quad (1)$$

where $F \equiv (\mathcal{F} - \mathcal{F}_o)/(\bar{\rho} k_B T L^d)$, \mathcal{F}_o is the free energy functional at constant density, $\bar{\rho}$ is the average number density, k_B is Boltzmann's constant, T is temperature, $L \equiv \sqrt{2|\hat{C}_4|/|\hat{C}_2|}$, C_i is the i point direct correlation function of the reference liquid state, $B^\ell \equiv 1 - \bar{\rho}\hat{C}_0$, $B^s \equiv \bar{\rho}(\hat{C}_2)^2/4|\hat{C}_4|$, $\vec{r} = \vec{x}/L$ and v accounts for the lowest order contribution from C_3 . $n = (\rho - \rho_L)/\rho_L$ is the scaled number density, where ρ is the local density variable and $\rho_L = \bar{\rho}$ is the liquid number density. Classical density functional theory has been used to examine surface melting [2, 19], but not grain boundary melting, presumably due to the complexity of the solid-solid interface and the more demanding system size requirements.

The dynamics are given in dimensionless form by

$$\frac{\partial n}{\partial \tau} = \nabla^2 \frac{\delta F}{\delta n} + \eta \quad (2)$$

where $\langle \eta(\vec{r}_1, \tau_1) \eta(\vec{r}_2, \tau_2) \rangle = M \nabla^2 \delta(\vec{r}_1 - \vec{r}_2) \delta(\tau_1 - \tau_2)$ and $M \equiv 3(\bar{\rho} L^d)^2$. This form imposes a constant density and is consistent with the canonical ensemble.

A semi-implicit pseudospectral algorithm was used to solve Eq. (2) in three dimensions with periodic boundary

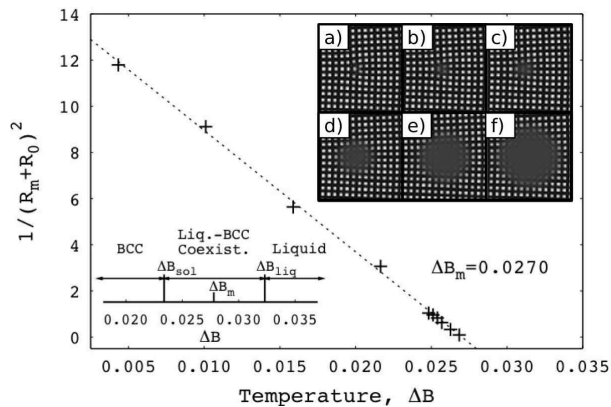


FIG. 1: Numerically measured local melt radius R_m around an edge dislocation in a bcc crystal as a function of temperature (units of lattice constant a , $\Delta B < 0.025$ values obtained by extrapolation of $\phi(\vec{r})$). $R_0 = 0.2812a$ is the zero temperature radius, determined by best fit. Inset: cross-sectional images of $n(x, y, z)$ from simulations at $\Delta B = 0.02165, 0.02511, 0.02569, 0.02627, 0.02656, 0.02685$ from a) to f), showing melting at a dislocation core.

conditions. The parameters used were $\Delta x = 0.976031$, $\Delta \tau = 0.5$, $B^s = \sqrt{3}/3$, $v = 3^{1/4}/2$, and $M = 0.002$. A system size $V = (512\Delta x)^3 = (56a)^3$ was used for the dislocation pair and 4° grain boundary pair, while $V = (256\Delta x)^3 = (28a)^3$ was used for all other grain boundary pairs, where $a = 8.9237$ is the bcc lattice constant. Finite size effects increase as θ decreases, but were found to be small for all grain boundaries studied. The gaussian width or mean square displacement (D) of each localized density peak was monitored as the temperature $\Delta B \equiv B^\ell - B^s$ was increased toward the melting point. The local crystallinity ϕ has been defined as $\phi(\vec{r}) = (D(\vec{r}) - D_X)/(D_L - D_X)$, where D_X is the equilibrium D of the crystal phase and D_L is that of the liquid phase. $\phi = 1/2$ specifies a liquid-solid interface.

The radius of melted region around a dislocation core R_m was first measured in this manner for an edge dislocation pair as the temperature was raised toward the bulk melting temperature ΔB_m . The results are shown in Fig. 1, where the data is plotted as $(R_m + R_0)^{-2}$ vs ΔB to demonstrate that R_m is consistent with a $(\Delta B_m - \Delta B)^{-1/2}$ form which will be derived later. R_0 is an offset related to the finite size of the dislocation core at zero temperature. The fit to this form predicts a bulk melting temperature $\Delta B_m = 0.0270$ which is in good agreement with the directly measured value of $\Delta B_m = 0.0278$. The upper inset of Fig. 1 shows melting around an edge dislocation as $\Delta B \rightarrow \Delta B_m$.

Figure 2 shows the progression of melting at 8° and 44° grain boundaries. Low angle boundaries were found to first melt radially at each dislocation core, until the melted regions of neighboring dislocations coalesce and a uniform wetting layer is formed along the boundary. Indi-

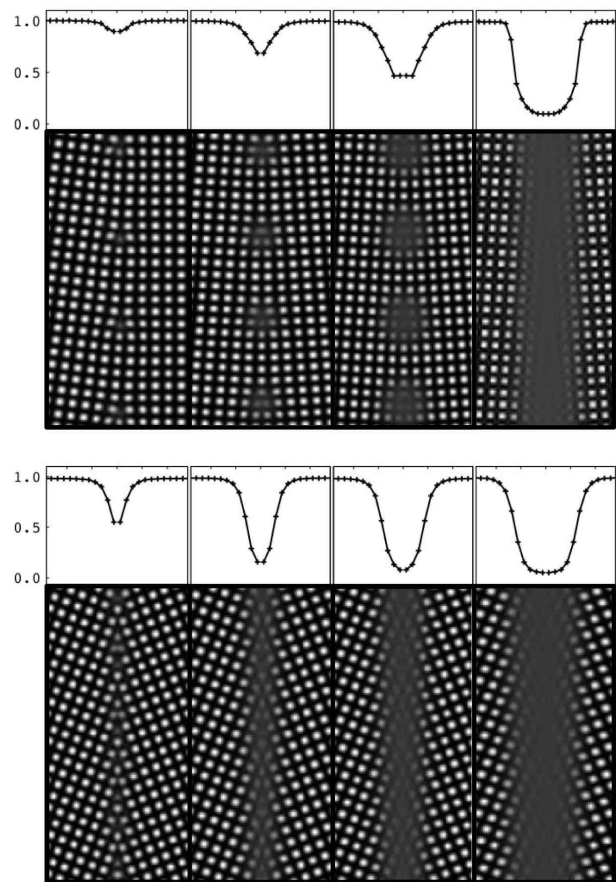


FIG. 2: Laterally averaged crystallinity parameter ϕ and cross-sections of $n(x, y, z)$ for 8° (upper) and 44° (lower) grain boundaries at $\Delta B = 0.02165, 0.02627, 0.02656, 0.02685$ and $\Delta B = 0.02425, 0.02468, 0.02540, 0.02656$ from left to right, respectively.

vidual dislocations cannot be distinguished in high angle boundaries, and melting in this case was found to proceed by uniform disordering along the boundary rather than by local radial melting. Interfacial roughening due to thermal fluctuations is negligible in all simulations presented here.

The dependence of the width of the wetting layer (or the liquid volume fraction of the system) on ΔB is shown in the inset of Fig. 3 for various grain boundary angles. In all cases the width remains narrow and the boundary relatively dry until above the solidus, at which point a discontinuous jump is observed at some characteristic wetting temperature ΔB_{wet} . The dependence of ΔB_{wet} on θ is shown in the main plot of Fig. 3. The fit lines will be discussed in the following, though the axes of the plot reveal already that our predicted form will be $\Delta B_{wet} \propto \sin^2 \theta$.

Based on these simulation results, we have developed a theory of dislocation-driven melting, which is easily extended to low angle grain boundaries. The low angle results are shown to remain accurate for all but the high-

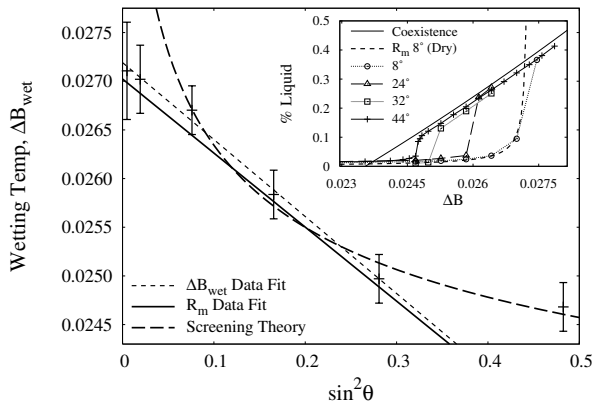


FIG. 3: Grain boundary wetting temperature vs. $\sin^2 \theta$. Fit lines are discussed in the text. Inset: Liquid volume fraction vs ΔB for a various grain boundaries. The dotted line corresponds to the liquid volume fraction predicted for the 8° boundary based on Eq. (5) only (ignoring coexistence).

est θ where the dislocation spacing d reaches the order of the burger's vector b . A screening approximation for the spatial grain boundary energy is found to be more applicable for very large θ , with a gradual crossover taking place between these two regimes.

According to continuum elasticity [20], the radially averaged elastic energy density per length of dislocation line in a three-dimensional isotropic solid is $\bar{F}_{el} = \alpha\mu/R^2$, where μ is the shear modulus. For a screw dislocation $\alpha_s = b^2/4\pi^2$ and for an edge dislocation $\alpha_e = \alpha_s/(1 - \sigma)$ where σ is the Poisson ratio. If we assume this result to hold for a dislocation in the PFC model, at distances approaching the core region, then R_m can be directly calculated by determining the distance at which \bar{F}_{el} is sufficiently large to destabilize the crystalline phase, melting the dislocation core.

It will be assumed that n can be represented in a one mode approximation for a bcc lattice, i.e., $n(\vec{r}) = A(\cos qx \cos qy + \cos qx \cos qz + \cos qy \cos qz)$. Substituting n into Eq. (1) and minimizing with respect to q gives,

$$\Delta f^X = \frac{3}{8}\Delta B A^2 - \frac{v}{8}A^3 + \frac{45}{256}A^4 \quad (3)$$

where $\Delta f^X \equiv (F - F_L)/V$, F_L is the free energy of the liquid, $V = (2\pi/q)^3$, and $q_{min} = \sqrt{2}/2$. The shear modulus can be estimated in the one mode approximation by setting $n(x, y, z) \rightarrow n(x + \zeta y, y, z)$ and expanding F in ζ such that $F = F(\zeta = 0) + \mu\zeta^2 + \dots$. This procedure gives $\mu/k_B T L^2 \bar{\rho} = A^2 B^s/8$. The total (dimensionless) free energy of the system with a dislocation is then $\Delta f^X + \bar{F}_{el}/k_B T \bar{\rho} L^d$, which can be written

$$\Delta f = \frac{3}{8} \left(\Delta B + \frac{E}{\bar{R}^2} \right) A^2 - \frac{v}{8} A^3 + \frac{45}{256} A^4. \quad (4)$$

where $\bar{R} \equiv R/b$ and $E_s \equiv B^s/(12\pi^2)$, $E_e \equiv E_s/(1 - \sigma)$ for screw and edge dislocations respectively. Equation (4) indicates that the elastic energy 'shifts' the effective temperature ΔB by an amount E/\bar{R}^2 . The implication is that the liquid-solid transition is shifted and instead of occurring when $\Delta B = \Delta B_m$ occurs when $\Delta B + E/\bar{R}^2 = \Delta B_m$. Thus the premelt radius can be written

$$\bar{R}_m = \sqrt{E/(\Delta B_m - \Delta B)} \quad (5)$$

or $1/\bar{R}_m^2 = (\Delta B_m - \Delta B)/E$.

As shown in Fig. 1, this form is consistent with the simulation results for edge dislocation pairs, though the predicted slope ($-1/E_e$) is in error by a factor of nearly five. A more definitive test would require additional data very near ΔB_m , a region increasingly difficult to access due to system size requirements.

Extending this result to low angle boundaries, we can estimate the grain boundary wetting temperature ΔB_{wet} where neighboring dislocations coalesce by setting $\bar{R}_m = d/2 = 1/(2 \sin \theta)$. Substituting Eq. (5) for \bar{R}_m gives

$$\Delta B_{wet} = \Delta B_m - 4E \sin^2 \theta \quad (6)$$

which is in good agreement with the data shown in Fig. 3. This result should lose accuracy as θ increases since the dislocation energies gradually deviate from the isolated dislocation result as $\theta \rightarrow \theta_{max}$. The agreement up to $\theta \simeq 32^\circ$ is somewhat unexpected as the superposition generally loses accuracy for $\theta \gtrsim 10^\circ$. The best fit line predicts $\Delta B_m = 0.0272$, again near the measured value.

The solid line in Fig. 3 corresponds to the fit line from Fig. 1, set equal to $1/(2 \sin \theta)$ and solved for ΔB_{wet} . The agreement here clearly indicates that the wetting of low and mid-angle grain boundaries is accurately described by the coalescence of radially melted regions around nearly isolated dislocations.

In the limit of large θ ($d \rightarrow 0$), the grain boundary energy becomes increasingly uniform along its length (see Fig. 2) and can no longer be described in terms of individual dislocations. We expect that elastic fields at long distances are screened by closely spaced dislocations, giving rise to exponentially decaying spatial grain boundary energy. Indeed, direct analysis of free energy data from simulations indicates that such an exponential form is qualitatively correct. Solving for ΔB_{wet} using $\bar{F}_{el} \propto e^{-x/b}$ rather than $\bar{F}_{el} \propto 1/R^2$ gives $\Delta B_m - \Delta B_{wet} \propto e^{-f(\theta)}$. This is the form of the wide dashed line in Fig. 3, which appears to be more appropriate for large θ .

Some comments concerning the influence of liquid-solid coexistence and the canonical ensemble (i.e., conserved density) on grain boundary melting may be helpful at this point. The equilibrium state for a simple system with a grain boundary is most generally either dry if $F_{gb} < 2F_{ls} + \ell(\bar{F}_L - \bar{F}_X)$ or wet if $F_{gb} > 2F_{ls} + \ell(\bar{F}_L - \bar{F}_X)$, where F_{gb} is the grain boundary energy, F_{ls} is the energy

of a liquid-solid interface, and ℓ is the width of the liquid region in the wet state. If the wet state becomes favorable below the melting temperature, then a grain boundary wetting transition occurs. In the canonical ensemble as examined here, the effects of liquid-solid coexistence and the subsequent shifts in density of the two phases above the solidus ΔB_{sol} modify this heuristic argument. Now ΔB_m , the temperature at which $\bar{F}_L = \bar{F}_X$, is straddled by a coexistence region. As $\Delta B \rightarrow \Delta B_m$ the system first encounters a solidus above which some volume fraction of liquid will minimize the overall \bar{F} . For the grain boundary pair geometry, the equilibrium state above ΔB_{sol} is one with a uniform volume of liquid occupying each boundary region. Therefore, an equilibrium first order wetting transition will occur at ΔB_{sol} as long as the grain size is not excessively small. Above ΔB_{sol} , the liquid layer width will be controlled by coexistence rather than local defect energies, since the elastic fields of the grains largely decouple ($\bar{F}_{el} \rightarrow 0$) upon wetting.

The results presented here show no wetting or strong premelting for $\Delta B \leq \Delta B_{sol}$, and the equilibrium wetting transition is not observed. Instead, a θ -dependent discontinuous transition from the metastable dry boundary state to the equilibrium wet state occurs at $\Delta B_{sol} < \Delta B_{wet} < \Delta B_m$, as shown in the inset of Fig. 3. This is because the wetted state is not nucleated in observable times until R_m has grown sufficiently large to coalesce and the free energy barrier approaches zero. The dislocations and/or grain boundaries act as nucleation sites for the liquid above ΔB_{sol} , creating well-defined nonequilibrium paths from the metastable dry state to the F minimizing wet state (which all must conserve ρ).

The condition for wetting in the canonical ensemble involves the grain size L_g , such that wetting can be suppressed to temperatures above ΔB_{sol} when L_g is finite. The condition can be written $F_{gb} + L_g \Delta F_X > 2F_{ls} + \ell \Delta F_C$ where $\Delta F_X = \bar{F}_X[\bar{\rho}] - \bar{F}_X[\rho_X]$ and $\Delta F_C = \bar{F}_L[\rho_L] - \bar{F}_X[\rho_X]$. Here $\ell = (\rho_X - \bar{\rho})/(\rho_X - \rho_L)$, $\bar{\rho}$ is the conserved system density, and ρ_X and ρ_L are the shifted coexistence densities of the solid and liquid phases, respectively. For $\Delta B \leq \Delta B_{sol}$, if we assume that $\Delta F_X = 0$ and $\rho_L = \rho_X = \bar{\rho}$ (this is not the case when premelting is strong below ΔB_{sol}), we recover the original inequality $F_{gb} > 2F_{ls} + \ell(\bar{F}_L - \bar{F}_X)$ and L_g is not a significant factor. In the limit $L_g \rightarrow \infty$, the wetting condition will always be satisfied for $\Delta B > \Delta B_{sol}$ and the equilibrium transition occurs at ΔB_{sol} . As L_g decreases, the equilibrium wetting transition is shifted to higher ΔB .

Two-dimensional systems show qualitatively similar results to those presented above. Preliminary simulations have also been conducted in the grand canonical ensemble (i.e., non-conserved density), where the above complications with liquid-solid coexistence due to den-

sity conservation can be avoided. Initial results indicate that there is no strong wetting transition in this case, as the atoms near grain boundaries continuously delocalize toward ΔB_m but do not liquify and decouple the grains until above ΔB_m .

JB would like to acknowledge support from the Richard H. Tomlinson and Carl Reinhardt Foundations of McGill University and thank Maria Kilfoil, Dan Vernon, Zhi-Feng Huang, Katsuyo Thornton, and Nilima Nigam for useful discussions. KRE acknowledges support from the National Science Foundation under Grant No. DMR-0413062. MG acknowledges support from the Natural Sciences and Engineering Research Council of Canada, and *le Fonds québécois de la recherche sur la nature et les technologies*.

-
- [1] D. W. Oxtoby, *Nature* **347**, 725 (1990).
 - [2] H. Löwen, *Phys. Rep.* **237**, 249 (1994).
 - [3] A. M. Alsayed, M. F. Islam, J. Zhang, P. J. Collings, and A. G. Yodh, *Science* **309**, 1207 (2005).
 - [4] T. Hsieh and R. Balluffi, *Acta Metall.* **37**, 1637 (1989).
 - [5] E. Budke, T. Surholt, S. I. Prokofjev, L. S. Shvindlerman, and C. Herzig, *Acta Mater.* **47**, 385 (1999).
 - [6] S. Divinski, M. Lohmann, C. Herzig, B. Straumal, B. Baretzky, and W. Gust, *Phys. Rev. B* **71**, 104104 (2005).
 - [7] K. Author and D. Demianczuk, *Acta Metall.* **23**, 1149 (1975).
 - [8] T. Watanabe, S.-I. Kimura, and S. Karashima, *Philos. Mag. A* **49**, 845 (1984).
 - [9] T. Nguyen, P. S. Ho, T. Kwok, C. Nitta, and S. Yip, *Phys. Rev. B* **46**, 6050 (1992).
 - [10] J. Q. Broughton and G. H. Gilmer, *Phys. Rev. Lett.* **56**, 2692 (1986).
 - [11] R. Kikuchi and J. W. Cahn, *Phys. Rev. B* **21**, 1893 (1980).
 - [12] M. Tang, W. C. Carter, and R. M. Cannon, *Phys. Rev. B* **73**, 024102 (2006).
 - [13] A. E. Lobkovsky and J. A. Warren, *Physica D* **164**, 202 (2002).
 - [14] M. Rappaz, A. Jacot, and W. J. Boettinger, *Metall. and Mater. Trans. A* **33A**, 1 (2002).
 - [15] K. R. Elder and M. Grant, *Phys. Rev. E* **70**, 051605 (2004).
 - [16] K. R. Elder, N. Provatas, J. Berry, P. Stefanovic, and M. Grant, *Phys. Rev. B* **75**, 064107 (2007).
 - [17] T. V. Ramakrishnan and M. Yussouff, *Phys. Rev. B* **19**, 2775 (1979).
 - [18] Y. Singh, *Phys. Rep.* **207**, 351 (1991).
 - [19] R. Ohnesorge, H. Löwen, and H. Wagner, *Phys. Rev. E* **50**, 4801 (1994).
 - [20] P. M. Chaikin and T. C. Lubensky, *Principles of Condensed Matter Physics* (Cambridge University Press, Cambridge, UK, 1995).